

Aalborg Universitet



The influence of multiple cognitive workload levels of an exergame on dorsal attention network connectivity at the source level

Ghani, Usman; Niazi, Imran; Signal, Nada; Kumari, Nitika; Amjad, Imran; Haavik, Heidi; Taylor, Denise

Published in:
Physiology & Behavior

DOI (link to publication from Publisher):
[10.1016/j.physbeh.2024.114628](https://doi.org/10.1016/j.physbeh.2024.114628)

Creative Commons License
CC BY-NC-ND 4.0

Publication date:
2024

Document Version
Accepted author manuscript, peer reviewed version

[Link to publication from Aalborg University](#)

Citation for published version (APA):

Ghani, U., Niazi, I., Signal, N., Kumari, N., Amjad, I., Haavik, H., & Taylor, D. (2024). The influence of multiple cognitive workload levels of an exergame on dorsal attention network connectivity at the source level. *Physiology & Behavior*, 284, Article 114628. <https://doi.org/10.1016/j.physbeh.2024.114628>

General rights

Copyright and moral rights for the publications made accessible in the public portal are retained by the authors and/or other copyright owners and it is a condition of accessing publications that users recognise and abide by the legal requirements associated with these rights.

- Users may download and print one copy of any publication from the public portal for the purpose of private study or research.
- You may not further distribute the material or use it for any profit-making activity or commercial gain
- You may freely distribute the URL identifying the publication in the public portal -

Take down policy

If you believe that this document breaches copyright please contact us at vbn@aub.aau.dk providing details, and we will remove access to the work immediately and investigate your claim.

The Influence of multiple cognitive workload levels of an exergame on Dorsal Attention Network Connectivity at the Source Level

Usman Ghani ^{a,b*}, Imran Niazi ^{a,b,c}, Nada Signal ^b, Nitika Kumari ^a,
Imran Amjad ^a, Heidi Haavik ^a, Denise Taylor ^b

a. Centre for Chiropractic Research, New Zealand College of Chiropractic, Auckland, New Zealand

b. Department of health and sciences, Auckland University of Technology (AUT), New Zealand

c. Department of Health Science and Technology, Aalborg University, Aalborg, Denmark

Abstract

This study investigates how adding a cognitive task on a balance board (exergame) affects connectivity in the dorsal attention network (DAN) during an exergame task. Healthy young adults performed a soccer ball-moving task by tilting a balance board with their feet while their brain activity was measured using electroencephalography (EEG). In this exergame, the speed of obstacles in front of the goal manipulated the cognitive workload. Higher speed means a higher cognitive workload. The study found significant changes in functional connectivity within DAN regions, specifically in the alpha band. During the shift from easy to medium cognitive task, we observed a significant increase in connectivity ($p = 0.0436$) between the right inferior temporal (ITG R) and the Left middle temporal (MTG L). During the transition from easy to hard cognitive tasks, strengthened interactions ($p = 0.0324$) between inferior temporal (ITG) and parsopercularis (pOPPER) were found. This suggests that the proposed balanceboard-based exergame enhances the functionality of specific brain regions, such as ITG and MTG regions, and improves connectivity in the frontal cortex. We also found a correlation between brain activity and performance data, highlighting that increased cognitive workload resulted in decreased performance and heightened frontal alpha activity. These findings align with research suggesting that adding cognitive games to physical activity-based tasks in rehabilitation programs can boost brain activity, resulting in improved decision-making and visual processing skills. This information can help clinicians tailor rehabilitation methods that target specific brain regions.

Keywords: Dorsal Attention Network (DAN); Cognitive workload; Electroencephalogram (EEG), Exergame, and Phase lag index (PLI)

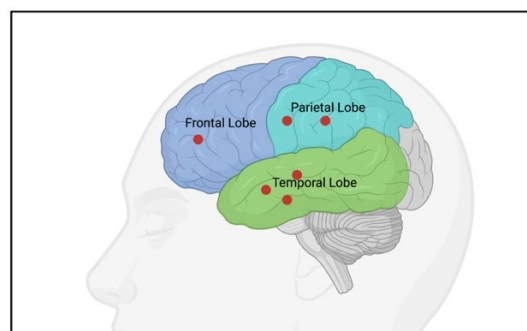
1. Introduction

Neurorehabilitation focuses on the recovery and rehabilitation of individuals who have suffered from brain injury, disease or other neurological disorders (Levine et al., 2011). In recent years, there has been a growing interest in using cognitive workload evaluation in neurorehabilitation, particularly for developing effective rehabilitation strategies (Tunik et al., 2013). The cognitive workload of patients is an important factor to consider, as it can impact the effectiveness of neurorehabilitation programs (Ghani et al., 2020a; Mark et al., 2004). Although several objective measures of cognitive workload evaluation with EEG have been proposed (Ghani et al., 2020b; Ghani et al., 2021; Zhou et al., 2022), it remained unclear how different brain regions communicate under different workload levels or how the underlying mechanisms work. Such information can help develop more robust methods of cognitive workload evaluation. Therefore, in this study, more emphasis was placed on connectivity analysis and source

43 localisation in cognitive workload evaluation, as it can provide important insights into the
44 neural mechanisms underlying cognitive function and help develop more effective
45 rehabilitation strategies for patients (Schoffelen & Gross, 2009).

46 Connectivity analysis is a powerful method for examining the communication and
47 collaboration between different brain regions during complex cognitive tasks (Šverko et al.,
48 2022). Connectivity analysis can be done at the sensor level (Duan et al., 2021) or the source
49 level (Hassan & Wendling, 2018). Due to volume conduction, EEG signals at the sensor level
50 express a complex mixture of overlapping signals from other EEG sensors (Rutkove, 2007).
51 Therefore, EEG source reconstruction is considered more robust for calculating functional
52 connectivity between the sources (Hassan & Wendling, 2018). Irrespective of sensor and
53 source-based approaches, two widely used approaches to measure functional connectivity are
54 1) Coherence and 2) Phase lag index (PLI). Coherence, a widely used approach, evaluates
55 linear associations between signals by measuring the consistency of phase differences between
56 two signals over time (Briels et al., 2020). In contrast, PLI assesses non-linear relationships by
57 quantifying the asymmetry of the distribution of phase differences between signals, focusing
58 on true interactions and avoiding spurious correlations due to volume conduction effects (Briels
59 et al., 2020). Both coherence and PLI have been employed in attention-related studies, offering
60 valuable insights into the communication between brain regions under varying levels of
61 attention and cognition (Mateos et al., 2022; Ueda et al., 2020). Thus, these techniques can
62 enhance our understanding of the intricate dynamics of the brain's functional connectivity
63 during cognitive tasks.

64 Recently, PLI has been used extensively to study the dorsal attention network (DAN), a
65 network of brain regions critical for attention and cognitive control (Dixon et al., 2017; Rohr
66 et al., 2017). The DAN includes brain regions such as the superior parietal lobe and the frontal
67 eye fields, which are involved in spatial attention and eye movements (Szczepanski et al.,
68 2013). These brain regions are shown in **Figure 1**. Understanding how these regions
69 communicate with each other and with other brain networks is crucial for understanding how
70 the brain supports attention and cognition. One important question is how the DAN operates
71 under different levels of cognitive workload. Previous research has shown that the DAN is
72 activated during tasks requiring high attention, such as visual search and working memory tasks
73 (Corbetta & Shulman, 2002). However, it is still unclear how the network adapts to changing
74 levels of cognitive demand and how this affects its communication patterns. In this study, we
75 used an exergame as a task with multiple levels of cognitive workload to see how the
76 connectivity of source reconstructed EEG changes in DAN with variation in cognitive
77 workload.



78

79

Figure 1: Brain (sagittal right view) with DAN regions Created with BioRender.com

80 Exergames, which combine physical activity and cognitive challenges, have emerged as a
81 useful tool for investigating cognitive processes during complex tasks (Maillot et al., 2012). In
82 this context, the current study aimed to examine the impact of cognitive workload changes on
83 the connectivity within the DAN during an exergame. We will use the data collected during
84 our previous work, which validated that the exergame provided three distinct levels of
85 cognitive workload (Ghani et al., 2021). In this previous study, EEG was employed to measure
86 brain activity in twenty-four healthy adults who completed an exergame task that involved
87 moving a soccer ball into a highlighted goal by tilting a balance board with their feet. The task's
88 cognitive workload was manipulated by adjusting the speed of obstacles in front of the goal,
89 creating three distinct workload levels (more details on the task can be found at (Ghani et al.,
90 2021)). Participants were presented with three cognitive workload levels (easy, medium, and
91 hard) and task-irrelevant auditory tones to generate event-related potentials (ERPs). In our
92 previous studies, we looked at the amplitude change of these ERPs with cognitive workload
93 and found that the amplitude of these ERPs decreased with an increase in cognitive workload
94 (Ghani et al., 2020b; Ghani et al., 2021). This suggested an increase in attention towards the
95 task and a decrease in attention towards the auditory tone with an increase in cognitive
96 workload. In this study, we wanted to look at the change in connectivity between brain regions
97 with an increase in cognitive workload. Based on the literature and previous findings, we
98 hypothesised that the connectivity between brain regions will increase with increased cognitive
99 workload. We will also correlate performance data collected during the study, such as the
100 number of goals scored and subjective ratings of task difficulty, with changes in brain activity
101 (PLI).

102 **2. Method**

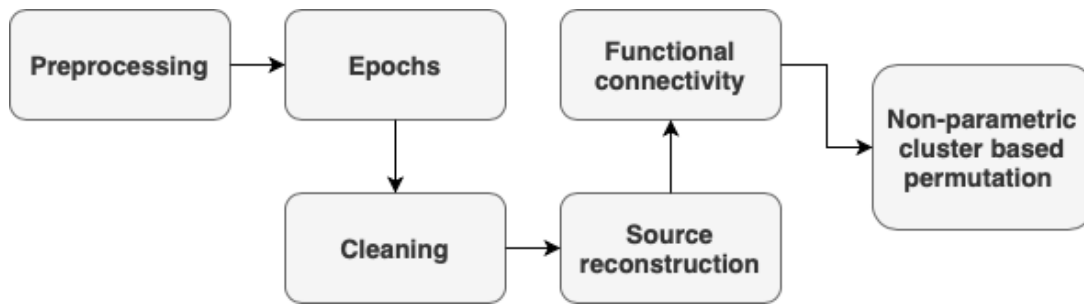
103 **2.1. Participants and task**

104 Twenty-four young, healthy adults (11 females, age range: 20–30 years, mean age: 25 ± 3.4
105 years) were recruited via advertisements through university networks and word of mouth. The
106 task was a tilt-ball game that participants played while standing on a balance board (for details
107 on the study procedure, see (Ghani et al., 2021)).

108 **2.2. EEG data processing**

109 The overall flow graph of the EEG data processing for the study is shown in Figure 2. The EEG
110 data was acquired using a 64-channel Brainwave EEG cap coupled with a REFA amplifier
111 (TMSi, Twente, Netherlands) at a sampling rate of 2,048 Hz. The recordings were obtained
112 from 64 scalp sites, following the 10-20 electrode system (Homan et al., 1987), with the ground
113 electrode situated at AFz and both mastoids (M1 and M2) employed as reference points.
114 Electrode impedance was consistently maintained below 10 k Ω . Additionally, online filter
115 settings were adjusted to a range of DC-100 Hz, incorporating a 50 Hz notch filter during the
116 raw data acquisition process. The raw EEG data were preprocessed offline using EEGLAB
117 (version 14.1.1) (Delorme & Makeig, 2004) and ERPLAB (version 6.1.4) (Lopez-Calderon &
118 Luck, 2014) running on MATLAB (2015b) (The MathWorks, Inc, Natick, MA, United States).

119 For the EEG preprocessing, 62 electrodes were re-referred to achieve a common average
120 reference excluding the two mastoids. We used the PREP pipeline (version 0.55.1) (Bigdely-
121 Shamlo et al., 2015) to remove and interpolate bad channels and line noise.



122

123

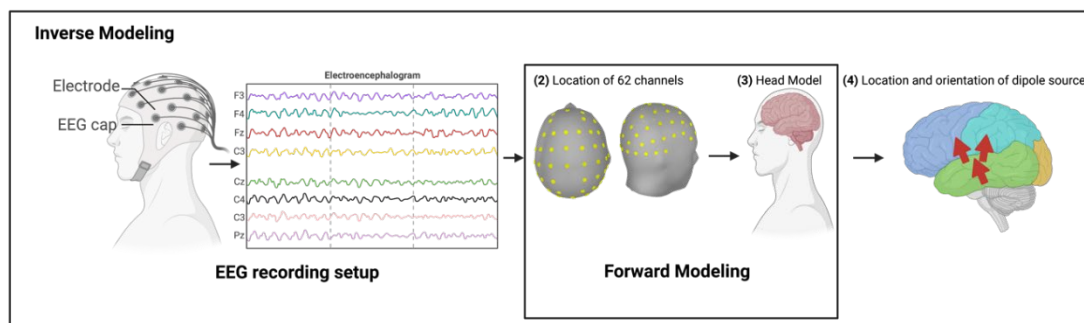
Figure 2: EEG data processing pipeline

124

125 After running the PREP pipeline, epochs were extracted from -200 to 1500 ms to the stimulus
 126 and corrected baseline using the pre-stimulus period. The bad channels were visually marked
 127 from the data before running the independent component analysis (ICA). Custom-written ICA
 128 code was then used to remove bad components from the data. The data obtained after epoching
 129 and ICA were subjected to the ERPLAB artifact detection algorithm of moving window
 130 threshold (Lopez-Calderon & Luck, 2014). A 200 ms window width and a 100 ms step were
 131 defined with a threshold of ± 100 μV . The epochs in which the signal exceeded ± 100 μV on
 132 any channel were rejected. This preprocessed data (interpolated to full channels) was then
 133 loaded into Brainstorm for source estimation.

134 **2.3. Source reconstruction**

135 EEG source reconstruction was performed using Brainstorm (Tadel, 2011) in MATLAB
 136 R2022a. Source reconstruction is a method used in neuroscience to estimate the location and
 137 activity of underlying neural sources based on measurements obtained from multiple sensors
 138 or electrodes (Hämäläinen & Ilmoniemi, 1994). Using advanced mathematical models and
 139 algorithms, source reconstruction can provide a more comprehensive understanding of brain
 140 activity by identifying the specific regions and networks involved in specific tasks or
 141 behaviours (Friston, 2011). There are two main problems in EEG source reconstruction:
 142 forward modelling and inverse modelling, both dependent on each other for accurate source
 143 reconstruction (Sadleir & Argibay, 2007). Forward modelling involves the human head,
 144 including its scalp, skull, cortex, and electromagnetic properties (Hassan & Wendling, 2018).
 145 The inverse modelling problem uses the information about cortical activity from forward
 146 modelling to identify the most likely locations and strengths (Sadleir & Argibay, 2007). In
 147 subsequent sub-sections, forward and inverse modelling will be explained in detail. The overall
 148 process of source reconstruction is shown in Figure 3.



149

150

Figure 3: Source reconstruction pipeline

151 2.3.1. Forward Modelling

152 This section outlines the forward modelling process for EEG source reconstruction. Our goal
153 was to determine the location and orientation of EEG sensors relative to the cortical source,
154 which required defining the location and orientation of current dipole fields (Sadleir &
155 Argibay, 2007; Tadel et al., 2011). We accomplished this by placing source dipoles on a voxel
156 grid space approximating the cortical space, ensuring they were oriented perpendicular to the
157 cortex. We used the symmetric boundary element method (Open MEEG BEM) to model the
158 dipoles for all subjects (Tadel et al., 2011). We employed a default generic head model from
159 Brainstorm May 2023, which featured 15,000 vertices and a three-layer compartment (scalp,
160 skull, and brain). Tissue conductivities were set based on a previous study by R.J Sadlier
161 (Sadleir & Argibay, 2007): scalp = 1, skull = 0.0125, and brain = 1. We calculated the forward
162 model after defining the 64 electrode locations (including ref: M1 and M2) on the scalp using
163 the 10-20 electrode placement system and the Colin27 Neuroscan Quick-Cap 64.

164 2.3.2. Inverse Modelling

165 The inverse problem is a technique used in neuroscience to estimate activity from the brain
166 based on measurements taken from electroencephalography (EEG) sensors (Schoffelen &
167 Gross, 2009). This technique solves an underdetermined and ill-posed problem where the
168 number of estimated sources exceeds the number of electrodes used to record the data. To
169 achieve a solution, the method of minimum-norm estimation is utilised, which involves
170 applying a linear kernel to the spatial data at each point in time (Grech et al., 2008). This
171 technique estimates cortical current source densities by minimising the overall power of the
172 estimated sources while using an identity matrix as the noise covariance matrix (Tadel et al.,
173 2011). However, the minimum-norm estimate tends to locate sources in the superficial regions
174 of the cortex, leading to inaccurate results. We, therefore, used the standardised low-resolution
175 brain electromagnetic tomography (sLORETA) method to adjust current density maps of
176 source dipoles, representing them as normalised current densities perpendicular to the cortex
177 (Brunovsky et al., 2008). To efficiently assess functional connectivity, we grouped the high-
178 resolution sources based on the Desikan Killiany atlas, which defines 68 regions of interest
179 (ROIs) on the cortex surface. Averaging the time series within each ROI, we formed a [ROIs
180 x time] matrix. As suggested by the literature, we also flipped the sign of dipoles with opposite
181 directions before averaging to prevent activity cancellation. This approach enabled accurate
182 estimation of brain activity and an understanding of how different brain regions are connected.

183 2.4. Functional Connectivity

184 2.4.1. Dorsal Attention Network

185 DAN is a neural network involved in attentional control and spatial processing. Table 1 shows
186 key brain regions, subregions within the DAN, and their common abbreviations taken from
187 (Kabbara et al., 2017).

188

189 *Table 1: Brain sub-regions within DAN*

Brain Regions	Abbreviations	Brain Regions
cAUDalanteriorcingulate L	cACC L	Cingulate
cAUDalanteriorcingulate R	cACC R	Cingulate
inferiortemporal L	ITG L	Temporal

inferiortemporal R	ITG R	Temporal
middletemporal L	MTG L	Temporal
middletemporal R	MTG R	Temporal
parsopercularis L	pOPPER L	Frontal
parsopercularis R	pOPPER R	Frontal
parsorbitalis L	pORB L	Frontal
parsorbitalis R	pORB R	Frontal
parstriangularis L	pTRI L	Frontal
parstriangularis R	pTRI R	Frontal

190

191 Before the functional connectivity calculation, the DAN was derived from the sources only
 192 considering brain regions within this network.

193 **2.4.2. Phase Lag Index**

194 PLI is a measure of connectivity that quantifies asymmetry based on the phase difference
 195 distribution between two signals, denoted as 'x(t)' and 'y(t)'. We first calculated the average
 196 phase difference using Equation (1) to compute the PLI. This requires obtaining the signal's
 197 phase information, which is derived from the phase of the ratio between the signal's Hilbert
 198 transform and the signal itself.

$$199 \quad PLI_{x,y} = \left| \frac{1}{N} \sum_{t=1}^N \text{sign}[\sin(\phi_x(t) - \phi_y(t))] \right| \quad (1)$$

200 The resulting phase difference can be positive, negative, or zero, depending on the sign. The
 201 phase differences were evaluated across a specific window to determine the PLI and the
 202 calculation was performed over N total samples contained within that window. This process
 203 enabled us to quantify the extent of connectivity and asymmetry between the signals, providing
 204 valuable insights into the functional interactions of brain regions.

205 This study divided the data into narrow-band signals using a 4th-order Butterworth filter before
 206 PLI computation. This step allowed us to extract specific frequency bands: alpha (7.5–12.5
 207 Hz), beta (12.5–30 Hz), and gamma (30–40 Hz), based on the ranges reported in the study
 208 Newson and Thiagarajan (2019). The computation of PLI was done between every
 209 reconstructed EEG source signal in a pair. The result of the computed PLI lies in the interval
 210 from zero to one, where zero indicates no connectivity, and one indicates maximum
 211 connectivity between signals. After the computation of PLI between every source pair, the PLI
 212 data were stored in an adjacency matrix of dimension 12 x 12 with zeros along the diagonal,
 213 giving a symmetric square matrix corresponding to the number of sources. We had three 12 x
 214 12 adjacency matrices corresponding to easy, medium and hard within alpha in the DAN. We
 215 used non-parametric cluster-based permutations to find significant source pairs when we
 216 compared different workload levels.

217 **2.4.3. Non-parametric cluster-based permutation**

218 We employed a non-parametric cluster-based permutation test to handle the multiple
 219 comparison problem and control the familywise error (Maris & Oostenveld, 2007). Using a
 220 within-study design, this test compared the calculated PLI values within the adjacency matrices
 221 across multiple workload levels (easy vs medium, easy vs hard, and medium vs hard). The non-
 222 parametric cluster-based permutation test was conducted using the Field Trip toolbox provided
 223 by the Donders Institute, Brain, Cognition, and Behavior in Nijmegen, the Netherlands. For
 224 each pairwise comparison (easy vs. medium, easy vs. hard, medium vs. hard), we calculated

225 cluster-level statistics. The largest cluster-level statistic served as the critical t-value for
226 determining significant clusters. To create a null distribution, we conducted 5000 permutations
227 by randomly shuffling the data labels for each comparison. We then recalculated cluster-level
228 statistics for each permutation, reflecting the expected distribution of results under the null
229 hypothesis of no differences in functional connectivity between conditions.

230 The *p*-value for each observed cluster was computed as the proportion of permutations where
231 the cluster-level statistic was more extreme (either larger or smaller, depending on the
232 directionality) than the observed cluster-level statistic. A significant positive cluster (+cluster)
233 indicated increased functional connectivity, whereas a significant negative cluster (-cluster)
234 indicated decreased functional connectivity in one condition. This analysis allowed us to
235 identify brain regions where functional connectivity significantly changed between conditions,
236 shedding light on the impact of cognitive workload on brain network interactions. The results
237 were visualised within the cortex using EEGNET version 1 ([Hassan et al., 2015](#)); where
238 statistically significant results were illustrated as red spheres representing the brain region and
239 connecting lines representing statistical dependencies from the functional connectivity metrics
240 between brain regions ([Hassan et al., 2015](#)).

241 **2.4.4. Correlation Analysis**

242 The brain regions within the DAN were categorised into three main regions: Frontal, Temporal,
243 and Cingulate, based on the assignments outlined in Table 1. We then calculated the mean PLI
244 values for each of the three main brain regions (Frontal, Temporal, and Cingulate) for every
245 participant to examine the relationship between task performance (goals scored and ratings)
246 and brain activity (PLI values). After that, we performed Pearson correlation analyses to
247 explore the connections between goals scored, ratings, and the mean PLI values in each brain
248 region. This correlation analysis was aimed to determine how brain activity patterns
249 corresponded to performance and perceived task difficulty across different brain regions.

250 **3. Results**

251 **3.1. Cluster-based Permutation:**

252 We analysed EEG data from 24 subjects. The analysis revealed that higher cognitive workload
253 resulted in increased functional connectivity within the DAN in various brain regions within
254 the alpha frequency band calculated from the PLI.

255 A non-parametric cluster-based permutation test compared the PLI values between different
256 workload levels (easy, medium, and hard). In this test, a cluster was defined as a set of spatially
257 adjacent connections that showed significant differences between these workload levels. The
258 test controlled for multiple comparisons and familywise errors. Four positive clusters were
259 found when comparing easy and medium workload levels ($t = 3.945$, $p = 0.0436$), indicating
260 increased connectivity. Similarly, six positive clusters were observed when comparing easy
261 and hard levels ($t = 7.43$, $p = 0.0324$), indicating increased connectivity. However, no
262 significant clusters were observed when comparing medium to hard workload levels for both
263 positive ($t = 2.82$, $p = 0.6399$) and negative ($t = -2.18$, $p = 0.9$) clusters. The reported t-statistic
264 and p-value for each condition in Table 2 represent the largest cluster's t-statistic and associated
265 p-value derived from the cluster-level permutation test, ensuring that they reflected the most
266 significant change within the identified clusters.

267
268
269

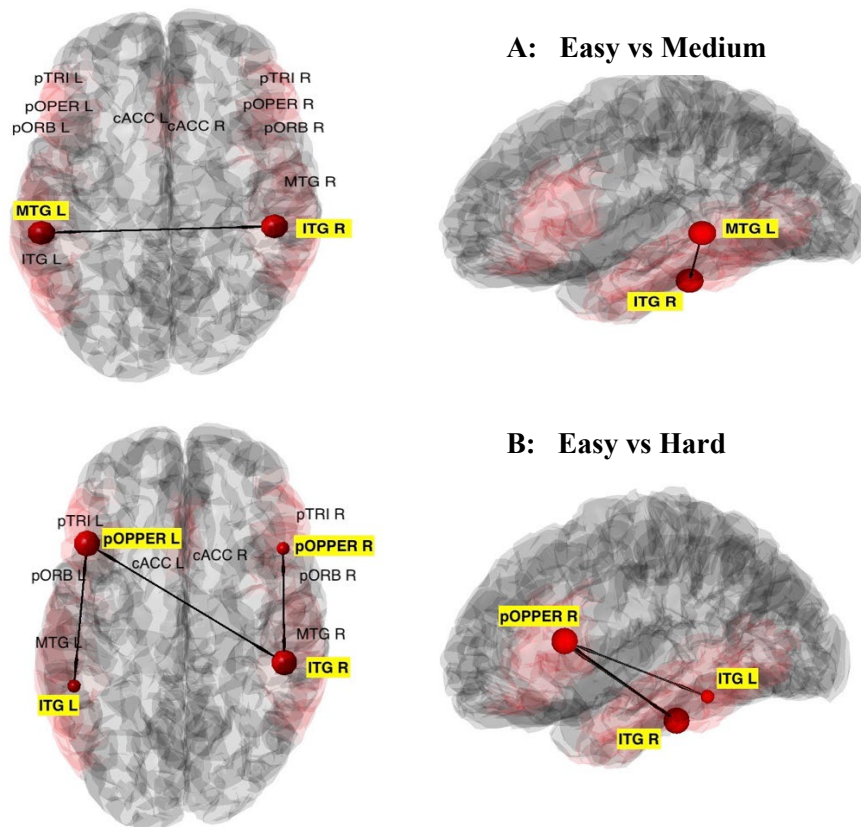
Table 2: The non-parametric cluster-based permutation test results comparing functional connectivity within the dorsal attention network for PLI. The PLI metric was compared for Easy vs Medium, Easy vs Hard, and Medium vs Hard within the Alpha band. Positive an

Condition	+Clusters	t-value	p-value	-Clusters	t-value	p-value
Easy vs Medium	4	3.945	0.0436	0	-	-
Easy vs Hard	6	7.43	0.0324	0	-	-
Medium vs Hard	4	2.82	0.6399	4	-2.18	0.9

270

271 Within identified significant clusters, several brain regions were involved, and Figure 4
272 illustrates these brain regions whose functional connectivity from the PLI metric was
273 significantly increased from (A) easy to medium and (B) easy to hard. The results were
274 visualised at the cortex level with the connected brain regions using EEGNET (version 1)
275 (Hassan et al., 2015) and custom-written MATLAB code for the circular graph plots to better
276 understand the significant changes found. Furthermore, a circular graph highlighted
277 connectivity (PLI values) between the brain regions. This circular graph is shown in Figure 5.

278



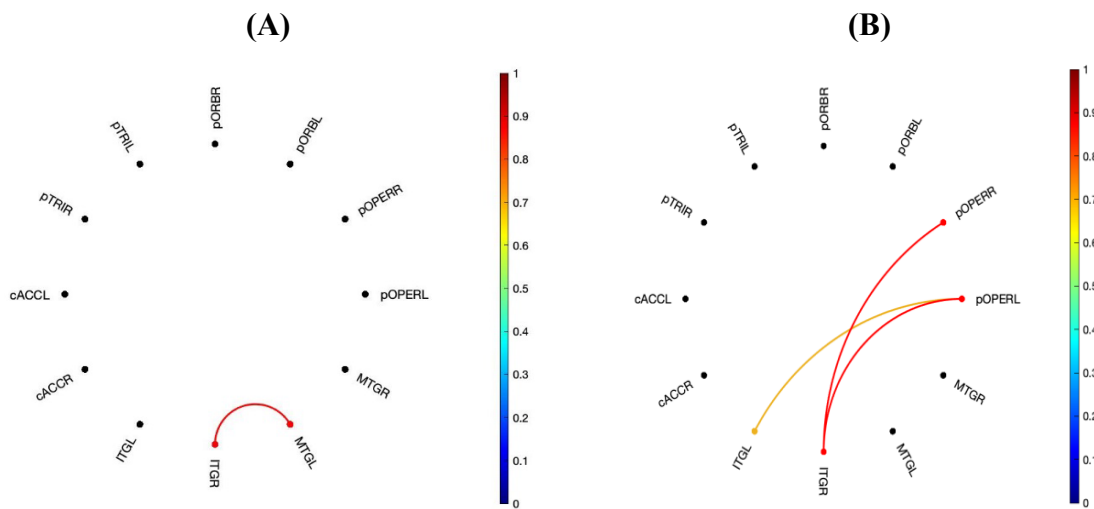
279
280
281
282
283
284
285
286

Figure 4: Alpha functional connectivity changes in brain regions when transitioning from **A:** Easy to Medium, and **B:** Easy to Hard. The cortex visualisation displays networks and connectivity, with red highlighted areas indicating the DAN and labelled brain regions. Significant results are represented by bold labels and yellow highlights, with red dots representing brain regions and lines showing functional connectivity via PLI metrics. Mentioned brain regions are cAUDalantteriorcingulate L (cACC L), cAUDalantteriorcingulate R (cACC R), inferiortemporal L (ITG L), inferiortemporal R (ITG R), middletemporal L (MTG L), middletemporal R (MTG R), parsopercularis L (pOPPER L), parsopercularis R (pOPPER R), parsorbitalis L (pORB L), parsorbitalis R (pORB R), parstriangularis L (pTRI L), parstriangularis R (pTRI R).

287
288
289
290

The functional connectivity matrix PLI increased significantly in the alpha band in inferior temporal R (ITG R) and middle temporal L (MTG L) brain regions within the DAN as we moved from easy to medium. Similarly, PLI increase in the following brain regions was observed as we moved from easy to hard cognitive workload. 1) inferiortemporal L (ITG L)

291 and parsopercularis L (pOPPER L), 2) inferiortemporal R (ITG R) and parsopercularis R
 292 (pOPPER R), and 3) inferior temporal R (ITG R) and parsopercularis L (pOPPER L). These
 293 interactions with corresponding effect sizes (cohen's d) are shown in Table 3.



294 **Figure 5:** The circular graph shows PLI connectivity between brain regions A) Easy vs Medium and B) Easy vs
 295 Hard. A higher PLI value means higher connectivity.

296 3.2. Correlation Analysis

297 A series of Pearson correlation analyses were performed to investigate the connections between
 298 Goals, Ratings, and PLI across three brain regions: Cingulate, Frontal, and Temporal. **Goals**
 299 **vs PLI:** For the Goals and PLI analysis, the Cingulate region showed a weak positive
 300 correlation ($r = 0.09, p = 0.561$). The Frontal region exhibited a moderate negative
 301 correlation, $r = -0.48, p < 0.001$. The Temporal region had a weak negative correlation ($r =$
 302 $-0.06, p = 0.698$.) **Ratings vs PLI:** In the Ratings and PLI analysis, the Cingulate region
 303 displayed a very weak positive correlation ($r = 0.06, p = 0.683$). The Frontal region showed a
 304 moderate to strong positive correlation ($r = 0.63, p < 0.001$). The Temporal region
 305 demonstrated a weak positive correlation ($r = 0.28, p = 0.052$). These results are shown in Table
 306 4 and Figure 6.

307 *Table 3: Effect size (Cohen's d) for significant clusters within the alpha band. For easy vs medium, inferiortemporal R (ITG*
 308 *R) and middletemporal L (MTG L). For easy vs hard, inferiortemporal R (ITG R), inferior temporal L (ITG L), parsopercularis*
 309 *L (pOPPER L)*

Condition	Regions	Condition 1	Condition 2	Cohen's d
Easy vs Hard		Easy	Hard	
	ITG L - pOPPER L	0.05	0.1754	0.42
	ITG R - pOPPER R	0.04	0.08	0.17
	ITG R - pOPPER L	0	0.28	-
Easy vs Medium		Easy	Medium	
	ITG R - MTG L	0.01	0.13	0.32

310

311

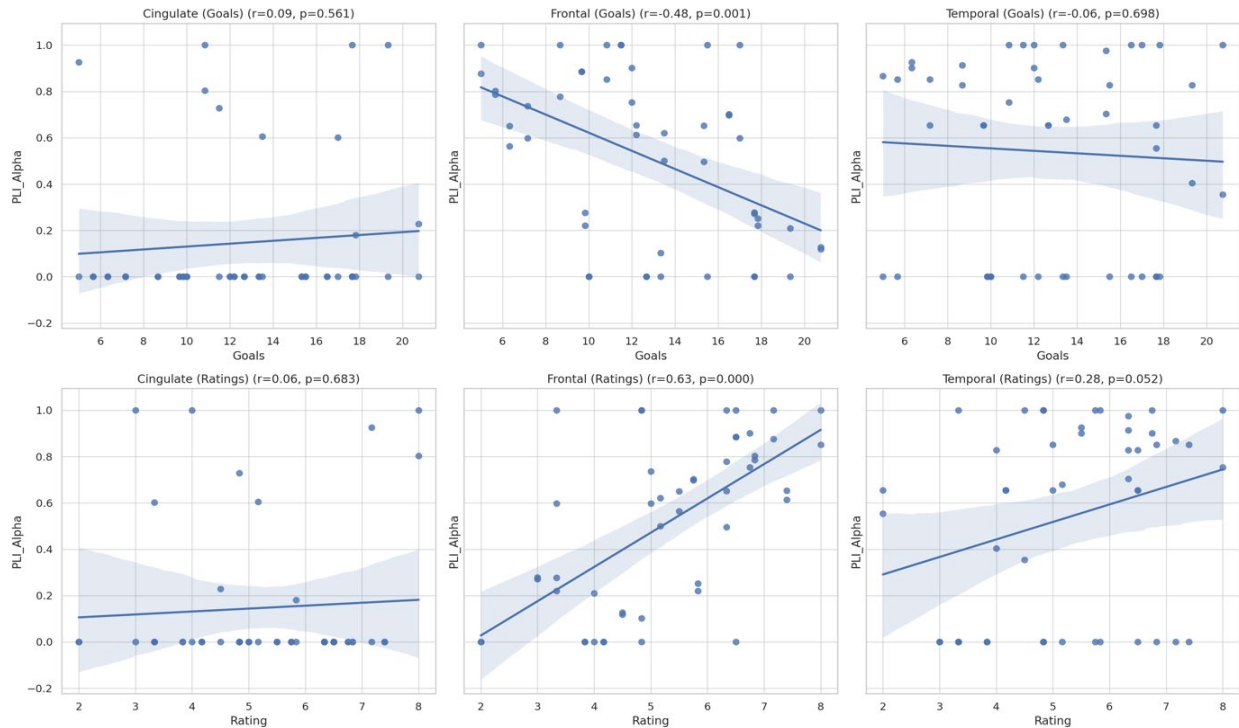
312 *Table 4: Performance vs Brain data (Correlation analysis)*

Brain Regions	Correlation	Pearson Correlation (r)	p-value
Frontal*	PLI vs Goals	-0.48	<0.001*
	PLI vs Ratings	0.63	<0.001*

Cingulate	PLI vs Goals	0.09	0.561
	PLI vs Ratings	0.06	0.683
Temporal	PLI vs Goals	-0.06	0.698
	PLI vs Ratings	0.28	0.052

313

Correlation between Goals/Ratings and PLI_Alpha across Brain Regions



314

315 *Figure 6: Correlation analysis of performance data with the brain data (PLI).*

316 4. Discussion

317 This study investigated how varying cognitive workload levels affect neural dynamics during
 318 an exergame task. Building upon previous research showing that the amplitude of N100 ERPs
 319 decreases as cognitive workload increases (Ghani et al., 2020a, 2020b; Kok, 2001), our study
 320 explored the connectivity changes based on the PLI applied to sources within the Dorsal
 321 Attention Network (DAN). During the shift from easy to medium cognitive workload, we
 322 observed a significant increase in connectivity within the alpha band between inferiortemporal
 323 R (ITG R) and middletemporal L (MTG L) within the DAN. On the other hand, during the
 324 transition from easy to hard cognitive workload, several significant changes in alpha band
 325 connectivity were observed within the DAN. These included the strengthened interactions
 326 between inferiortemporal L (ITG L) and parsopercularis L (pOPPER L), as well as the
 327 increased connectivity between parsopercularis R (pOPPER R) and inferiortemporal R (ITG
 328 R), and lastly, the heightened connectivity between parsopercularis R (pOPPER R) and
 329 inferiortemporal L (ITG L). furthermore, A correlation analysis revealed a negative correlation
 330 between performance and brain activity, as well as a positive correlation between perceived
 331 difficulty and brain activity.

332 We found significant changes only within the alpha frequency band. The absence of significant
 333 findings in the other frequency bands, such as beta and gamma bands, aligns with some studies
 334 that suggest task-specific and context-dependent variations in EEG responses (Molteni et al.,

335 2008). For example, Coelli et al. (2015) reported increased beta activity with cognitive
336 workload and concentration, but these effects were not universally observed across all tasks or
337 cognitive demands, a finding also supported by Molteni et al. (2008). Therefore, the exergame
338 used in our study often requires motor coordination, cognitive processing, and attentional
339 control (Fitzgerald et al., 2010), eliciting a different pattern of neural activation, predominantly
340 reflected in the alpha band and not in the other frequency bands. Furthermore, the alpha band
341 has been shown to be associated with attentional processes (Klimesch, 1997), which could be
342 highly engaged during the exergame tasks. Hence, It's plausible that the nature of the exergame
343 encouraged participants to allocate attention and resources to the task, resulting in significant
344 changes in the alpha band activity. Within the alpha band, multiple brain regions were involved
345 in this attention allocation as the cognitive workload increased. Understanding the functionality
346 of different brain regions is essential for gaining a more detailed interpretation of the results.

347 ITG R and MTG L are part of the temporal lobe, predominantly involved in visual processing
348 and perception (Kravitz et al., 2013; Mesgarani et al., 2014). The temporal lobe plays a crucial
349 role in processing complex visual stimuli, object recognition, and semantic memory, making it
350 highly relevant to the exergame task used in our study (Ghani et al., 2021). As the exergame
351 involved an increased speed of obstacles, participants encountered more intricate and rapidly
352 changing visual stimuli during a medium cognitive workload compared to the easy one.
353 Consequently, ITG R was more engaged in detailed visual feature processing and object
354 recognition. At the same time, MTG L played a role in integrating visual information and
355 extracting semantic meaning from the stimuli. The heightened connectivity between these
356 visual processing regions within the DAN during medium cognitive workload reflects their
357 concerted effort to manage the increase in cognitive workload of the exergame.

358 The increased connectivity between ITG L and pOPPER L during hard cognitive workload is
359 noteworthy, as ITG L is implicated in object recognition and visual processing (Vlcek et al.,
360 2020). At the same time, pOPPER L is associated with cognitive control processes and
361 decision-making (Fedorenko et al., 2013; Kravitz et al., 2013). This heightened connectivity
362 indicates a coordinated engagement of these regions in allocating attentional resources and
363 strategic decision-making to optimise task performance under higher cognitive demands.
364 Similarly, the observed increase in DAN connectivity between pOPPER R and ITG R further
365 supports the network's extensive interactions to facilitate attentional control during challenging
366 cognitive tasks (Capotosto et al., 2009). The interaction between pOPPER R and ITG R
367 involves integrating cognitive control processes and visual information processing, enabling
368 effective task engagement and performance during hard cognitive workloads. Lastly, the
369 heightened connectivity between pOPPER R and ITG L highlights the dynamic and
370 interconnected nature of the DAN in managing higher cognitive demands.

371 When comparing medium workload with hard workload, our results did not show significant
372 differences in connectivity. This lack of significant results could be due to several factors. One
373 possible explanation is the ceiling effect, where participants' cognitive capabilities might have
374 been maxed out during the medium workload, leaving little room for further significant
375 increases during the hard workload. Additionally, the neural mechanisms underlying medium
376 and hard cognitive workloads might involve similar brain regions and connectivity patterns,
377 making it challenging to detect distinct changes. Overall, These results reflected the network's
378 ability to adapt its connectivity flexibly to optimise cognitive performance during complex
379 tasks. The integrated efforts of these regions within the DAN suggest a coordinated system that
380 efficiently allocates attentional resources and facilitates cognitive processing in response to

381 varying levels of cognitive workload. We also performed a correlation analysis to examine how
382 brain activity relates to the performance metric (goals scored) and perceived difficulty (ratings).

383 **4.1. Correlation Analysis**

384 Our correlation analysis revealed that the number of goals scored decreased as task difficulty
385 increased (increasing PLI). This showed a significant negative correlation with the PLI in the
386 frontal region. These findings align with existing research suggesting that alpha oscillations in
387 the frontal cortex are associated with cognitive control and working memory load. In particular,
388 higher task difficulty has been linked to increased alpha activity in the frontal region, indicating
389 greater cognitive control and attentional demand. This is supported by studies showing that
390 frontal alpha activity tends to increase with greater task complexity and cognitive workload
391 (Katahira et al., 2018). Furthermore, alpha oscillations are known to impact cognitive processes
392 like attention and memory, which are crucial for effectively handling more challenging tasks
393 (Sadaghiani & Kleinschmidt, 2016). A significant positive correlation was also found between
394 subjective ratings and frontal PLI values, which again highlight heightened alpha activity in
395 the frontal region with the increased cognitive workload.

396 Overall, this study demonstrated that as the difficulty of the task in an exercise-based video
397 game increased, there was a higher phase lag index (PLI) in the alpha band between regions of
398 the DAN. Additional analysis also showed a connection between performance measures and
399 the PLI and reported that increased perceived difficulty rating was associated with heightened
400 alpha activity in the frontal brain region. These findings align with existing research, indicating
401 that frontal alpha oscillations are crucial for cognitive control and managing cognitive load.
402 The study underscores the significant role of the frontal cortex in adapting to varying cognitive
403 demands, highlighting how increased connectivity within this region supports enhanced
404 attentional control and task performance under challenging conditions. Recently, exergames
405 have been increasingly used in neurorehabilitation to accelerate recovery (Goble et al., 2014;
406 Hasselmann et al., 2015; Laufer et al., 2014). This study highlights the importance of adjusting
407 the difficulty level of exergames and how it can impact the engagement of brain resources,
408 involving more areas of the brain. Additionally, identifying the brain regions involved in
409 exergames can help clinicians optimise the task to expedite rehabilitation.

410 Although the study has revealed significant findings, it is important to consider certain
411 limitations. First, the present study focused on the DAN and its connectivity changes, but other
412 brain networks may also contribute to cognitive workload modulation and attentional control.
413 Future investigations employing a network-level approach could provide a more
414 comprehensive understanding of the brain's response to cognitive demands. Second, the
415 exergame task, while engaging, might not fully capture the complexity and ecological validity
416 of real-world cognitive tasks. Studies using a broader range of cognitive paradigms are needed
417 to generalise the findings to various cognitive activities. Moreover, it is essential to conduct a
418 thorough analysis of the connectivity between different brain regions and its impact on
419 performance measures.

420 **5. Conclusion**

421 Our study investigated neural dynamics linked to cognitive workload variations during an
422 exergame task, building on the established inverse relationship between N100 event-related
423 potential amplitudes and cognitive workload. By utilising connectivity analysis through the
424 PLI within the DAN, we aimed to uncover underlying mechanisms of cognitive workload

425 modulation. Our results revealed distinct DAN connectivity changes as participants shifted
426 from easy to medium and easy to hard cognitive workloads. During the easy-to-medium
427 transition, enhanced connectivity emerged between the inferior temporal R (ITG R) and
428 middle temporal L (MTG L), suggesting collaboration in processing complex visual stimuli.
429 Similarly, the easy-to-hard transition showed significant connectivity shifts within the DAN,
430 including strengthened interactions between the inferior temporal L (ITG L) and
431 pars opercularis L (pOPPER L), increased connectivity between the pars opercularis R
432 (pOPPER R) and inferior temporal R (ITG R), and heightened connectivity between the
433 pars opercularis R (pOPPER R) and inferior temporal L (ITG L), showcasing the network's
434 adaptability and attentional engagement under higher demands.

435 Correlation analysis revealed that as task difficulty increased, goal scoring decreased, with a
436 significant negative correlation between goals and frontal PLI. Subjective ratings were
437 positively correlated with frontal PLI, highlighting the role of frontal alpha oscillations in
438 managing cognitive load. These insights are valuable for optimising rehabilitation tasks and
439 suggest that future studies should integrate broader brain networks and behavioural measures
440 for a comprehensive understanding. Integrating behavioural measures with neural data would
441 enrich interpretations of connectivity changes relative to cognitive performance.

442

443

444 **6. Acknowledgment**

445 We thank Brain Research New Zealand (BRNZ) for sponsoring this research.

446 **7. Author Contribution statement**

447 **Usman Ghani:** Conceptualization, Formal analysis, Writing – original draft, Writing – review
448 & editing. **Imran Khan Niazi:** Conceptualization, Supervision, Funding acquisition, Writing
449 – review & editing. **Nada Signal:** Conceptualization, Supervision, Writing – review & editing.
450 **Nitika Kumari:** Writing – review & editing. **Imran Amjad:** Writing – review & editing.
451 **Heidi Haavik:** Conceptualization, Supervision, Funding acquisition, Writing – review &
452 editing. **Denise Taylor:** Formal analysis, Funding acquisition, Supervision, Writing – review
453 & editing.

454 **8. Data availability**

455 The authors will make the numerical data supporting this article's conclusions available without
456 undue reservation. Interested individuals can obtain this data by making a reasonable request
457 to the corresponding author, Usman Ghani. The Local Ethics Committee, adhering to local data
458 protection laws, does not allow sharing of individuals' raw data.

459

460

461 **9. References**

462

463 Bigdely-Shamlo, N., Mullen, T., Kothe, C., Su, K. M., & Robbins, K. A. (2015). The PREP pipeline:
464 standardized preprocessing for large-scale EEG analysis. *Front Neuroinform*, 9, 16.
465 <https://doi.org/10.3389/fninf.2015.00016>

466
467 Briels, C. T., Schoonhoven, D. N., Stam, C. J., de Waal, H., Scheltens, P., & Gouw, A. A. (2020,
468 2020/06/03). Reproducibility of EEG functional connectivity in Alzheimer's disease.
469 *Alzheimer's Research & Therapy*, 12(1), 68. <https://doi.org/10.1186/s13195-020-00632-3>

470
471 Brunovsky, M., Krajca, V., Diblikova, F., Bartos, A., Zavesicka, L., & Matousek, M. (2008, 2008/04/17).
472 Standardized low-resolution brain electromagnetic tomography (sLORETA) in the prediction
473 of response to cholinesterase inhibitors in patients with Alzheimer's disease. *Annals of*
474 *General Psychiatry*, 7(1), S277. <https://doi.org/10.1186/1744-859X-7-S1-S277>

475
476 Capotosto, P., Babiloni, C., Romani, G. L., & Corbetta, M. (2009, May 6). Frontoparietal cortex controls
477 spatial attention through modulation of anticipatory alpha rhythms. *J Neurosci*, 29(18), 5863-
478 5872. <https://doi.org/10.1523/jneurosci.0539-09.2009>

479
480 Coelli, S., Sclocco, R., Barbieri, R., Reni, G., Zucca, C., & Bianchi, A. (2015). *EEG-based index for*
481 *engagement level monitoring during sustained attention* (Vol. 2015).
482 <https://doi.org/10.1109/EMBC.2015.7318658>

483
484 Corbetta, M., & Shulman, G. L. (2002, Mar). Control of goal-directed and stimulus-driven attention in
485 the brain. *Nat Rev Neurosci*, 3(3), 201-215. <https://doi.org/10.1038/nrn755>

486
487 Delorme, A., & Makeig, S. (2004, Mar 15). EEGLAB: an open source toolbox for analysis of single-trial
488 EEG dynamics including independent component analysis. *J Neurosci Methods*, 134(1), 9-21.
489 <https://doi.org/10.1016/j.jneumeth.2003.10.009>

490
491 Dixon, M. L., Andrews-Hanna, J. R., Spreng, R. N., Irving, Z. C., Mills, C., Girn, M., & Christoff, K. (2017,
492 Feb 15). Interactions between the default network and dorsal attention network vary across
493 default subsystems, time, and cognitive states. *NeuroImage*, 147, 632-649.
494 <https://doi.org/10.1016/j.neuroimage.2016.12.073>

495
496 Duan, W., Chen, X., Wang, Y.-J., Zhao, W., Yuan, H., & Lei, X. (2021). Reproducibility of power spectrum,
497 functional connectivity and network construction in resting-state EEG. *Journal of Neuroscience*
498 *Methods*, 348, 108985.

499
500 Fedorenko, E., Duncan, J., & Kanwisher, N. (2013, Oct 8). Broad domain generality in focal regions of
501 frontal and parietal cortex. *Proc Natl Acad Sci U S A*, 110(41), 16616-16621.
502 <https://doi.org/10.1073/pnas.1315235110>

503
504 Fitzgerald, D., Trakarnratanakul, N., Smyth, B., & Caulfield, B. (2010). Effects of a wobble board-based
505 therapeutic exergaming system for balance training on dynamic postural stability and intrinsic
506 motivation levels. *journal of orthopaedic & sports physical therapy*, 40(1), 11-19.

507

508 Friston, K. (2011, Sep 15). Dynamic causal modeling and Granger causality Comments on: the
509 identification of interacting networks in the brain using fMRI: model selection, causality and
510 deconvolution. *NeuroImage*, 58(2), 303-305; author reply 310-301.
511 <https://doi.org/10.1016/j.neuroimage.2009.09.031>

512

513 Ghani, U., Signal, N., Niazi, I. K., & Taylor, D. (2020a, Nov). ERP based measures of cognitive workload:
514 A review. *Neurosci Biobehav Rev*, 118, 18-26.
515 <https://doi.org/10.1016/j.neubiorev.2020.07.020>

516

517 Ghani, U., Signal, N., Niazi, I. K., & Taylor, D. (2020b, Dec). A novel approach to validate the efficacy of
518 single task ERP paradigms to measure cognitive workload. *Int J Psychophysiol*, 158, 9-15.
519 <https://doi.org/10.1016/j.ijpsycho.2020.09.007>

520

521 Ghani, U., Signal, N., Niazi, I. K., & Taylor, D. (2021, 2021-September-08). Efficacy of a Single-Task ERP
522 Measure to Evaluate Cognitive Workload During a Novel Exergame [Original Research].
523 *Frontiers in Human Neuroscience*, 15. <https://doi.org/10.3389/fnhum.2021.742384>

524

525 Goble, D. J., Cone, B. L., & Fling, B. W. (2014, 2014/02/08). Using the Wii Fit as a tool for balance
526 assessment and neurorehabilitation: the first half decade of "Wii-search". *Journal of*
527 *NeuroEngineering and Rehabilitation*, 11(1), 12. <https://doi.org/10.1186/1743-0003-11-12>

528

529 Grech, R., Cassar, T., Muscat, J., Camilleri, K. P., Fabri, S. G., Zervakis, M., Xanthopoulos, P., Sakkalis,
530 V., & Vanrumste, B. (2008, 2008/11/07). Review on solving the inverse problem in EEG source
531 analysis. *Journal of NeuroEngineering and Rehabilitation*, 5(1), 25.
532 <https://doi.org/10.1186/1743-0003-5-25>

533

534 Hämäläinen, M. S., & Ilmoniemi, R. J. (1994, 1994/01/01). Interpreting magnetic fields of the brain:
535 minimum norm estimates. *Medical & Biological Engineering & Computing*, 32(1), 35-42.
536 <https://doi.org/10.1007/BF02512476>

537

538 Hassan, M., Shamas, M., Khalil, M., El Falou, W., & Wendling, F. (2015). EEGNET: An Open Source Tool
539 for Analyzing and Visualizing M/EEG Connectome. *PLOS ONE*, 10(9), e0138297.
540 <https://doi.org/10.1371/journal.pone.0138297>

541

542 Hassan, M., & Wendling, F. (2018). Electroencephalography Source Connectivity: Aiming for High
543 Resolution of Brain Networks in Time and Space. *IEEE Signal Processing Magazine*, 35(3), 81-
544 96. <https://doi.org/10.1109/MSP.2017.2777518>

545

546 Hasselmann, V., Oesch, P., Fernandez-Luque, L., & Bachmann, S. (2015, Sep 7). Are exergames
547 promoting mobility an attractive alternative to conventional self-regulated exercises for
548 elderly people in a rehabilitation setting? Study protocol of a randomized controlled trial. *BMC*
549 *Geriatr*, 15, 108. <https://doi.org/10.1186/s12877-015-0106-0>

550

551 Homan, R. W., Herman, J., & Purdy, P. (1987, Apr). Cerebral location of international 10-20 system
552 electrode placement. *Electroencephalogr Clin Neurophysiol*, 66(4), 376-382.
553 [https://doi.org/10.1016/0013-4694\(87\)90206-9](https://doi.org/10.1016/0013-4694(87)90206-9)

554
555 Kabbara, A., El Falou, W., Khalil, M., Wendling, F., & Hassan, M. (2017, 2017/06/07). The dynamic
556 functional core network of the human brain at rest. *Scientific Reports*, 7(1), 2936.
557 <https://doi.org/10.1038/s41598-017-03420-6>

558
559 Katahira, K., Yamazaki, Y., Yamaoka, C., Ozaki, H., Nakagawa, S., & Nagata, N. (2018). EEG Correlates
560 of the Flow State: A Combination of Increased Frontal Theta and Moderate Frontocentral
561 Alpha Rhythm in the Mental Arithmetic Task. *Front Psychol*, 9, 300.
562 <https://doi.org/10.3389/fpsyg.2018.00300>

563
564 Klimesch, W. (1997). EEG-alpha rhythms and memory processes. *International Journal of*
565 *Psychophysiology*, 26(1-3), 319-340.

566
567 Kok, A. (2001, May). On the utility of P3 amplitude as a measure of processing capacity.
568 *Psychophysiology*, 38(3), 557-577. <https://doi.org/10.1017/s0048577201990559>

569
570 Kravitz, D. J., Saleem, K. S., Baker, C. I., Ungerleider, L. G., & Mishkin, M. (2013, Jan). The ventral visual
571 pathway: an expanded neural framework for the processing of object quality. *Trends Cogn Sci*,
572 17(1), 26-49. <https://doi.org/10.1016/j.tics.2012.10.011>

573
574 Laufer, Y., Dar, G., & Kodesh, E. (2014). Does a Wii-based exercise program enhance balance control
575 of independently functioning older adults? A systematic review. *Clin Interv Aging*, 9, 1803-
576 1813. <https://doi.org/10.2147/cia.S69673>

577
578 Levine, B., Schweizer, T., O'Connor, C., Turner, G., Gillingham, S., Stuss, D., Manly, T., & Robertson, I.
579 (2011, 2011-February-17). Rehabilitation of Executive Functioning in Patients with Frontal
580 Lobe Brain Damage with Goal Management Training [Original Research]. *Frontiers in Human*
581 *Neuroscience*, 5. <https://doi.org/10.3389/fnhum.2011.00009>

582
583 Lopez-Calderon, J., & Luck, S. J. (2014, 2014-April-14). ERPLAB: an open-source toolbox for the analysis
584 of event-related potentials [Technology Report]. *Frontiers in Human Neuroscience*, 8.
585 <https://doi.org/10.3389/fnhum.2014.00213>

586
587 Maillot, P., Perrot, A., & Hartley, A. (2012, Sep). Effects of interactive physical-activity video-game
588 training on physical and cognitive function in older adults. *Psychol Aging*, 27(3), 589-600.
589 <https://doi.org/10.1037/a0026268>

590
591 Maris, E., & Oostenveld, R. (2007, 2007/08/15/). Nonparametric statistical testing of EEG- and MEG-
592 data. *Journal of Neuroscience Methods*, 164(1), 177-190.
593 <https://doi.org/https://doi.org/10.1016/j.jneumeth.2007.03.024>

594
595 Mark, A. G., Mark, A. G., Timothy, D. L., & Timothy, D. L. (2004). Challenge Point: A Framework for
596 Conceptualizing the Effects of Various Practice Conditions in Motor Learning. *Journal of Motor*
597 *Behavior*. <https://doi.org/10.3200/jmbr.36.2.212-224>

598

599 Mateos, D. M., Krumm, G., Arán Filippetti, V., & Gutierrez, M. (2022). Power Spectrum and
600 Connectivity Analysis in EEG Recording during Attention and Creativity Performance in
601 Children. *NeuroSci*, 3(2), 347-365. <https://www.mdpi.com/2673-4087/3/2/25>

602

603 Mesgarani, N., Cheung, C., Johnson, K., & Chang, E. F. (2014). Phonetic Feature Encoding in Human
604 Superior Temporal Gyrus. *Science*, 343(6174), 1006-1010.
605 <https://doi.org/doi:10.1126/science.1245994>

606

607 Molteni, E., Bianchi, A., Butti, M., Reni, G., & Zucca, C. (2008, 08/01). Combined Behavioral and EEG
608 Power Analysis in DAI Improve Accuracy in the Assessment of Sustained Attention Deficit.
609 *Annals of Biomedical engineering*, 36, 1216-1227. [https://doi.org/10.1007/s10439-008-9506-](https://doi.org/10.1007/s10439-008-9506-z)
610 [z](https://doi.org/10.1007/s10439-008-9506-z)

611

612 Newson, J. J., & Thiagarajan, T. C. (2019, 2019-January-09). EEG Frequency Bands in Psychiatric
613 Disorders: A Review of Resting State Studies [Review]. *Frontiers in Human Neuroscience*, 12.
614 <https://doi.org/10.3389/fnhum.2018.00521>

615

616 Rohr, C. S., Vinette, S. A., Parsons, K. A. L., Cho, I. Y. K., Dimond, D., Benischek, A., Lebel, C., Dewey, D.,
617 & Bray, S. (2017, Sep 1). Functional Connectivity of the Dorsal Attention Network Predicts
618 Selective Attention in 4-7 year-old Girls. *Cereb Cortex*, 27(9), 4350-4360.
619 <https://doi.org/10.1093/cercor/bhw236>

620

621 Rutkove, S. B. (2007). *Introduction to volume conduction* Clinical neurophysiology Primer pp 43-53.

622

623 Sadaghiani, S., & Kleinschmidt, A. (2016, Nov). Brain Networks and α -Oscillations: Structural and
624 Functional Foundations of Cognitive Control. *Trends Cogn Sci*, 20(11), 805-817.
625 <https://doi.org/10.1016/j.tics.2016.09.004>

626

627 Sadleir, R. J., & Argibay, A. (2007, Oct). Modeling skull electrical properties. *Ann Biomed Eng*, 35(10),
628 1699-1712. <https://doi.org/10.1007/s10439-007-9343-5>

629

630 Schoffelen, J. M., & Gross, J. (2009, Jun). Source connectivity analysis with MEG and EEG. *Hum Brain*
631 *Mapp*, 30(6), 1857-1865. <https://doi.org/10.1002/hbm.20745>

632

633 Šverko, Z., Vrankić, M., Vlahinić, S., & Rogelj, P. (2022). Complex Pearson Correlation Coefficient for
634 EEG Connectivity Analysis. *Sensors*, 22(4), 1477. [https://www.mdpi.com/1424-](https://www.mdpi.com/1424-8220/22/4/1477)
635 [8220/22/4/1477](https://www.mdpi.com/1424-8220/22/4/1477)

636

637 Szczepanski, S. M., Pinsk, M. A., Douglas, M. M., Kastner, S., & Saalmann, Y. B. (2013). Functional and
638 structural architecture of the human dorsal frontoparietal attention network. *Proceedings of*
639 *the National Academy of Sciences*, 110(39), 15806-15811.
640 <https://doi.org/doi:10.1073/pnas.1313903110>

641

642 Tadel. (2011). *Brainstorm*. <http://neuroimage.usc.edu/brainstorm>

643

644 Tadel, F., Baillet, S., Mosher, J. C., Pantazis, D., & Leahy, R. M. (2011). Brainstorm: a user-friendly
645 application for MEG/EEG analysis. *Comput Intell Neurosci*, 2011, 879716.
646 <https://doi.org/10.1155/2011/879716>

647
648 Tunik, E., Saleh, S., & Adamovich, S. V. (2013, Mar). Visuomotor discordance during visually-guided
649 hand movement in virtual reality modulates sensorimotor cortical activity in healthy and
650 hemiparetic subjects. *IEEE Trans Neural Syst Rehabil Eng*, 21(2), 198-207.
651 <https://doi.org/10.1109/tnsre.2013.2238250>

652
653 Ueda, R., Takeichi, H., Kaga, Y., Oguri, M., Saito, Y., Nakagawa, E., Maegaki, Y., & Inagaki, M. (2020,
654 Feb). Atypical gamma functional connectivity pattern during light sleep in children with
655 attention deficit hyperactivity disorder. *Brain Dev*, 42(2), 129-139.
656 <https://doi.org/10.1016/j.braindev.2019.11.001>

657
658 Vlcek, K., Fajnerova, I., Nekovarova, T., Hejtmanek, L., Janca, R., Jezdik, P., Kalina, A., Tomasek, M.,
659 Krsek, P., Hammer, J., & Marusic, P. (2020). Mapping the Scene and Object Processing
660 Networks by Intracranial EEG. *Front Hum Neurosci*, 14, 561399.
661 <https://doi.org/10.3389/fnhum.2020.561399>

662
663 Zhou, Y., Huang, S., Xu, Z., Wang, P., Wu, X., & Zhang, D. (2022). Cognitive Workload Recognition Using
664 EEG Signals and Machine Learning: A Review. *IEEE Transactions on Cognitive and*
665 *Developmental Systems*, 14(3), 799-818. <https://doi.org/10.1109/TCDS.2021.3090217>

666
667